Semiconducting and Electropolymerizable Liquid Crystalline Carbazole-Containing Porphyrin-Core Dendrimers

Alberto Concellón,[a,‡] Roberto Termine,[b] Attilio Golemme,*[,b] Pilar Romero,[a] Mercedes Marcos,[a] and José Luis Serrano*[,a,c]

The self-assembly of liquid crystals (LCs) is an important method to control the organization of single molecules into periodically nanostructured phases that have found applications in organic electronics. Herein, we report a new family of LC porphyrin-core dendrimers bearing carbazole moieties at the periphery of the dendrimer. These compounds are synthetic light-harvesting antennas, which exhibit intramolecular energy transfer from the carbazole moieties to the central porphyrin core. We also demonstrate that it is possible to deposit spherical polymeric nanoparticles on ITO electrodes *via* electrochemical crosslinking of peripheral carbazole units. Moreover, the porphyrin-core dendrimers exhibit discotic nematic phases with excellent film-forming properties and a strong tendency towards defect-free homeotropic alignment. Charge mobility studies reveal promising semiconductor properties with high hole mobility values. Therefore, such carbazole-containing LC dendrimers exhibit a unique combination of interesting properties, opening the way for the preparation of new optoelectronic materials.

Introduction

Liquid crystals (LCs) are fascinating soft materials that combine order and mobility from the molecular to the macroscopic level.[1] Due to their dynamic nature, LCs can potentially be used as new functional materials for electron, ion, and molecular transport, as well as for sensors, optics, and soft robotics.[2-6] Semiconducting LCs enable many organic electronic devices because they self-organize into nanostructured phases which provide properties similar to those of organic single crystals, while their dynamics is vital for the processability and the self-healing of structural defects.[7-9] Specifically, discotic LCs, composed of a rigid anisotropic core surrounded by several flexible alkyl chains, are the most promising candidates. Often, these disk-like molecules self-assemble into columns with a significant intermolecular overlap of the delocalized π-electrons, providing quasi-one-dimensional channels for charge transport.[10-15]

Molecular engineering can unlock further opportunities for the development of advanced multifunctional materials, since the self-organizing process of single moieties into periodically nanostructured mesophases can enhance the functions of such single molecules.[16-18] Thus, dendrimers are attractive candidates for the preparation of functional LCs. In these materials, the functional units are arranged in a highly congested environment, which leads to the formation of unique supramolecular organizations that are not achievable with conventional LCs.[19-21] Over the last few years, our group has exploited the structural versatility of dendrimers for the introduction of different functional units (donor-acceptor systems) in the dendritic structure. These functionalities self-assemble into a LC arrangement with a supramolecular order that facilitates charge transport. For example, we have recently obtained high charge mobility values out of *Janus* dendrimers containing carbazole electroactive moieties.[22] Interestingly, their semiconducting properties relied on the self-organization in columnar LC phases with a strong coaxial segregation within each column, wherein carbazole units filled the central column cross-section. Alternatively, we have described LC porphyrin-core dendrimers that have coumarin functional units around the porphyrin core.[23, 24] These dendrimers exhibited a discotic nematic phase with a pronounced tendency to defect-free homeotropic alignment. Moreover, charge mobility studies showed promising semiconductor properties with high hole mobility values (~ 1 $cm^2\ V^{-1}\ s^{-1}$).[24] However, the supramolecular structure of the discotic nematic phase does not exhibit any long-range columnar order, and this left an open question as to why such a high mobility is observed in a relatively disordered phase. Although the role played by a porphyrin-coordinated metal is certainly central for charge transport,[24] the contribution of the peripheral coumarin units is a question to be solved.

In order to clarify such issues, we describe here the synthesis and characterization of two porphyrin-core dendrimers with two different carbazole peripheral units (**Figure 1**). We decided the introduction of carbazole units at the periphery of the dendrimers, replacing coumarins, since carbazole derivatives have been widely used in organic electronics. We expect that this structural modification may shed light on the contribution of the peripheral units in charge transport properties. In order to advance in the structure-properties relationship, we have designed two different carbazole units, **Cz** and **PhCz**, which

[a.] *Instituto de Ciencia de Materiales de Aragón, Departamento de Química Orgánica, Universidad de Zaragoza-CSIC, 50009 Zaragoza, Spain.*
[b.] *LASCAMM CR-INSTM, CNR-NANOTEC Lab LiCryL, Dipartimento di Fisica, Universitá della Calabria, 87036 Rende, Italy. Email: a.golemme@unical.it*
[c.] *Instituto de Nanociencia de Aragón, Departamento de Química Orgánica, Universidad de Zaragoza, 50009 Zaragoza, Spain. Email: joseluis@unizar.es*
[‡] *Present address: Department of Chemistry, Massachusetts Institute of Technology, MA 02139, Cambridge, United States.*

differ in the connectivity of the carbazole unit. The aim of the work described here was to exploit the capability of these porphyrin-core dendrimers to self-assemble into LC organizations and evaluate their possible use in optoelectronics.

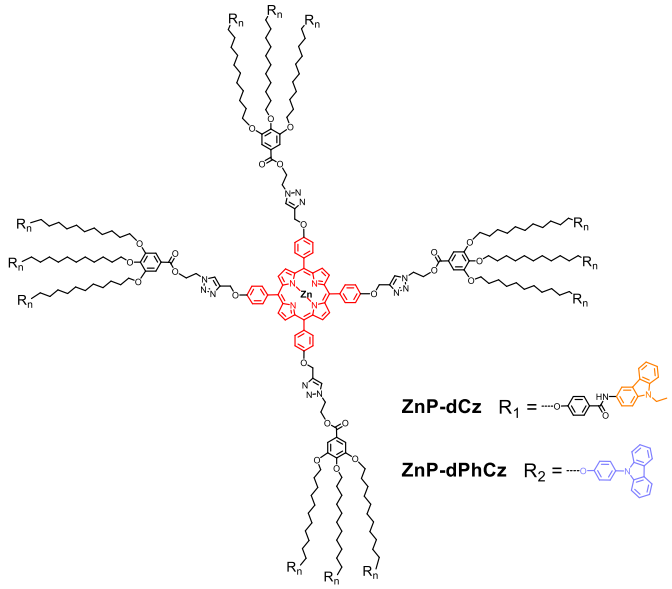

Figure 1. Chemical structure of the carbazole-containing porphyrin-core dendrimers.

Results and Discussion

Synthesis and Structural Characterization

The carbazole functional units (**2** and **7**) were prepared by the synthetic methodology described in **Scheme 1a**. Compounds **2** and **7** were then alkylated with 11-bromo-1-undecanol under standard Mitsunobu etherifications conditions. Subsequent etherification with methyl gallate under Williamson conditions yielded the methyl ester protected dendrons. Alkaline hydrolysis of the methyl ester group and subsequent esterification in the presence of ethanolazide resulted in **dCz** or **dPhCz.** (**Scheme 1b**).

The synthesis of the porphyrin-core dendrimers with carbazole units at the periphery (**ZnP-dCz** and **ZnP-dPhCz**) relies on the copper-catalyzed azide-alkyne 'click' cycloaddition (CuAAC) between tetraalkyne porphyrin (**ZnP**)[25] and azide-functionalized dendrons **dCz** and **dPhCz** (**Scheme 1b**). The CuAAC reaction was performed in THF/water at 40 ºC using $CuSO_4 \cdot 5H_2O$/sodium ascorbate as catalytic system, which has been widely used for the synthesis of dendritic structures with excellent coupling yields.[26-29] A slight excess of the azide dendron (1.5 equivalents per alkyne group) was employed to drive the coupling to completion and was removed by using an alkyne functionalized polystyrene resin. **ZnP-dCz** and **ZnP-dPhCz** were purified using standard column chromatography techniques and fully characterized. Evidence for the formation of the dendrimers was provided by the ^{1}H NMR spectra, where new peaks corresponding to the formed triazol ring appeared at 7.5–8.5 ppm (H_M in **Figure 2**) upon CuAAC coupling, and at 4.5–5.0 ppm corresponding to the methylenic protons linked to it (H_K and H_L in **Figure 2**). Further confirmation of the coupling was provided by MALDI-TOF mass spectroscopy. The MALDI-TOF mass spectra showed the expected peak and no other signals corresponding to dendrimers with a partial functionalization were detected (**Figure S7** and **S8**).

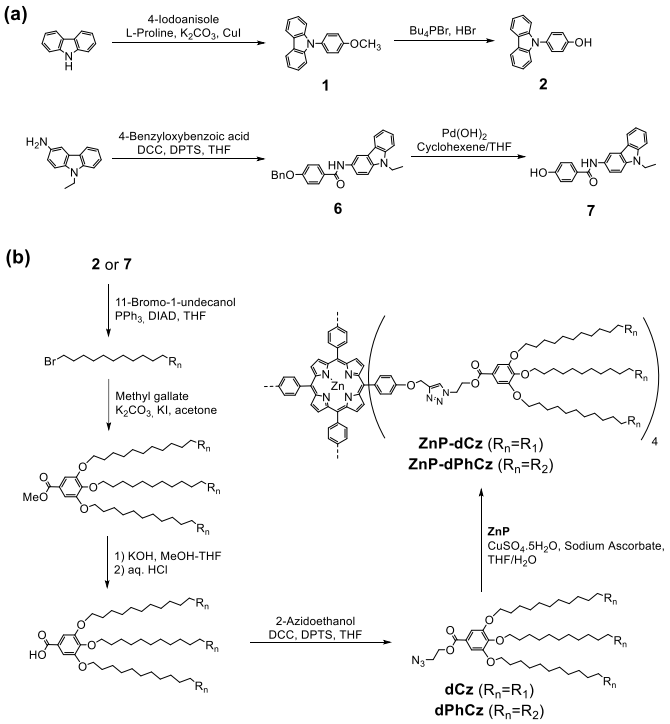

Scheme 1. Synthesis of the porphyrin-core dendrimers with peripheral carbazole moieties.

Thermal Stability and Liquid Crystalline Properties

The thermal stability of all the compounds was studied by thermogravimetric analysis (TGA). All compounds showed good thermal stability, with 2% weight loss temperatures ($T_{2\%}$) more than 150 °C above the clearing point (**Table 1**).

Table 1. Thermal Stability and Transition Temperatures.

	$T_{2\%}$ (°C)[a]	Phase transitions[b]
dCz	255	g 61 N 107[c] I
dPhCz	190	g -4 I
ZnP-dCz	320	g 82 N_D 155[c] I
ZnP-dPhCz	315	g 50 N_D 89[c] I

[a] Temperature at which 2% mass loss is detected by TGA. [b] DSC data of the second heating process at a rate of 10 °C/min. Temperatures are read at the maximum of the peak. g: glass, N: nematic mesophase, N_D: discotic nematic mesophase, I: isotropic liquid. [c] POM data.

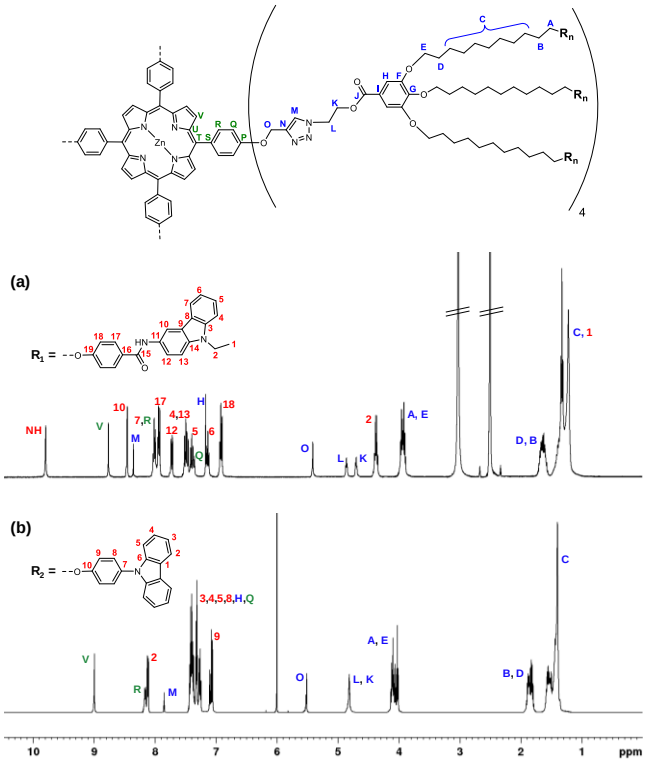

Figure 2. (a) ^{1}H NMR spectrum (500 MHz, DMSO-d_6, 353K) of **ZnP-dCz**, and **(b)** ^{1}H NMR spectrum (500 MHz, TCE-d_2, 373K) of **ZnP-dPhCz**.

Thermal transitions and liquid crystal properties were studied by polarized optical microscopy (POM), differential scanning calorimetry (DSC) and X-ray diffraction (XRD). The most relevant temperatures are gathered in **Table 1**. **dCz** exhibited an enantiotropic liquid crystal phase that was assigned as nematic on the basis of the birefringent textures with homeotropic domains observed by POM (**Figure S9a**). The absolute assignment of the mesophase was achieved by XRD studies. The XRD pattern showed diffuse scattering in the low-angle region, suggesting the absence of long-range positional order in the liquid crystal phase (**Figure S9b**). This kind of XRD pattern is consistent with a nematic mesophase. The other azide-functionalized dendron, **dPhCz**, behaved as a glassy material without showing liquid crystal properties.

Both porphyrin-core dendrimers (**ZnP-dCz** and **ZnP-dPhCz**) exhibited stable enantiotropic liquid crystalline mesophases, as observed by POM. Their DSC traces showed only a glass transition freezing the mesomorphic order at room temperature. The clearing temperatures were taken from POM observations because transition peaks were not detected in DSC curves. Under POM, both compounds had a high tendency to form large homeotropic domains. Therefore, the mesophase was observed on applying mechanical stress to the samples, showing birefringent textures (**Figure 3**). The nature of the mesophase was identified by XRD. The XRD patterns recorded for **ZnP-dCz** and **ZnP-dPhCz** showed diffuse scattering in the low-angle region (**Figure 3**). In the high-angle region, a broad diffuse scattering maximum was observed, which corresponds to an approximate distance of 4.5 Å. Such scattering is characteristic of liquid crystal phases and associated with the liquid-like order of the hydrocarbon chains. These XRD patterns, along with the POM textures are consistent with discotic nematic mesophases.

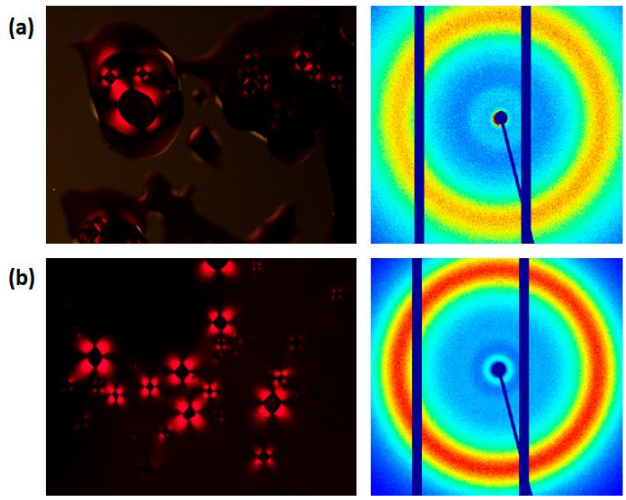

Figure 3. POM microphotographs (left) and XRD patterns (right) taken at room temperature for: **(a) ZnP-dCz**, and **(b) ZnP-dPhCz**.

Absorption and Emission properties

The UV-Vis absorption and fluorescence spectra of porphyrin-core dendrimers were collected on dilute solutions (10^{-5} to 10^{-7} M) and in thin films at room temperature. Relevant data are shown in **Table 2**. The UV-Vis absorption spectra of **ZnP-dCz** and **ZnP-dPhCz** in solution consisted of the porphyrin Soret (425 nm) and Q (500–700 nm) bands, and the characteristic carbazole π-π* (295-305 nm) and n-π* (340-370 nm) bands (**Figure 4a**). These absorption spectra were a combination of the spectra of the corresponding building blocks, and the presence of new bands was not observed. This result implies no conjugation effect between the two chromophores as the porphyrin core and the dendritic structure itself do not interfere with the absorption properties of the carbazole. The absorption bands for the porphyrin-core dendrimers in thin film exhibited a bathochromic shift of about 5 nm in relation to those in solution, due to an aggregation effect.

The fluorescence emission spectra of **ZnP-dCz** and **ZnP-dPhCz** obtained at an excitation wavelength (λ_{exc}) of 425 nm, consisted of two bands with a Q(0–1)-band at around 600 nm and a Q(0–2)-band at around 650 nm (**Figure 4b**). The fluorescence quantum yields (Φ_F) were also measured with tetraphenylporphyrin (Φ_F= 0.11 in benzene) as standard, obtaining low quantum yield values. In addition, the fluorescence was also collected in thin film, and compared to the data from DCM solutions, the emission peaks were red-shifted *ca.* 5 nm (**Figure 4b**).

Table 2. Photophysical data in solution and in thin film.

		λ_{abs} (nm) *Carbazole*	λ_{abs} (nm) *Soret band*	λ_{abs} (nm) *Q-bands*	λ_{em} (nm) *Carbazole*	λ_{em} (nm) *Q (0–1)*	λ_{em} (nm) *Q (0–2)*	Φ_F[a]	Φ_{FRET}
dCz	*THF*	300	–	–	389	–	–	–	–
	film	306	–	–	495	–	–	–	–
ZnP-dCz	*THF*	301	427	559, 600	389	609	650	0.10	16%
	film	306	436	562, 603	–[b]	610	654	–	–
dPhCz	*DCM*	295	–	–	385	–	–	–	–
	film	299	–	–	392	–	–	–	–
ZnP-dPhCz	*DCM*	294	424	551, 592	385	601	643	0.12	23%
	film	297	437	564, 606	–[b]	614	651	–	–

[a] The Φ_F values were calculated from DCM solutions with tetraphenylporphyrin (0.11 in benzene) as standard, excitation at 420 nm. [b] Not detectable.

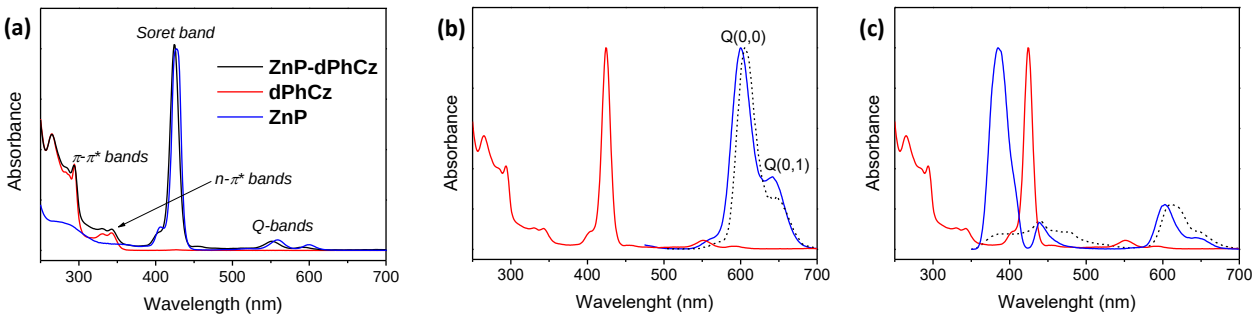

Figure 4. (a) Normalized UV-Vis absorption spectra in DCM solution of **dPhCz**, **ZnP** and **ZnP-dPhCz**. **(b, c)** Normalized UV-Vis absorption spectra in DCM solution (red line) and normalized emission spectra in DCM solution (blue line) and in thin film (dashed line) of **ZnP-dPhCz**: **(b)** λ_{exc} = 425 nm, and **(c)** λ_{exc} = 295 nm.

However, when peripheral carbazole units were excited selectively in their π-π* band (λ_{exc}= 295 nm), emissions from both the carbazole units and the porphyrin acceptor were observed (**Figure 4c**), thus demonstrating that fluorescence resonance energy-transfer (FRET) was facile but not quantitative in these systems. Light energy collected by peripheral carbazole chromophores is transferred to the porphyrin core (antenna effect), despite the low degree of overlap between the emission spectrum of the carbazole and the absorption spectrum of the porphyrin. The FRET efficiencies (Φ_{FRET}) are summarized in **Table 2** and were calculated by comparing the donor emission in the presence of the acceptor relative to that in the absence of the acceptor.[30-32] Moderate Φ_{FRET} values were obtained.

The fluorescence spectra at an excitation wavelength of λ_{exc} = 295 nm were also collected in thin film and compared to the data from solutions and almost no residual emission of the carbazole moieties was observed (**Figure 4c**). This result demonstrates that energy-transfer from carbazole units to the porphyrin core is more efficient in the thin film than in solution.[24]

Electrochemical Properties and Crosslinking of Carbazole Units

To study the possible application of these dendrimers in optoelectronics, it is important to investigate their electrochemical properties, which can be deduced from cyclic voltammetry (CV) experiments. **ZnP-dCz** and **ZnP-dPhCz** exhibited similar cyclic voltammograms, with one reduction wave corresponding to the porphyrin core, which is consistent with the electron acceptor character of this unit. Moreover, several oxidation processes were observed, and these are consistent with the porphyrin and carbazol electron donating moieties. The HOMO and LUMO energy values, calculated from the oxidation and reduction waves, are summarized in **Table 3**.

Table 3. Electrochemical parameters.

	E_{ox} (V)[a]	E_{HOMO} (eV)[b]	E_{red} (V)[a]	E_{LUMO} (eV)[b]
ZnP-dCz	0.82	–5.14	-1.36	–2.96
ZnP-dPhCz	0.59	–4.91	-1.38	–2.94

[a] Onset potential for the first oxidation/reduction process. [b] $E_{HOMO} = -(E_{ox} - E_{1/2,\ FOC} + 4.8)$ eV. $E_{LUMO} = -(E_{red} - E_{1/2,\ FOC} + 4.8)$ eV.

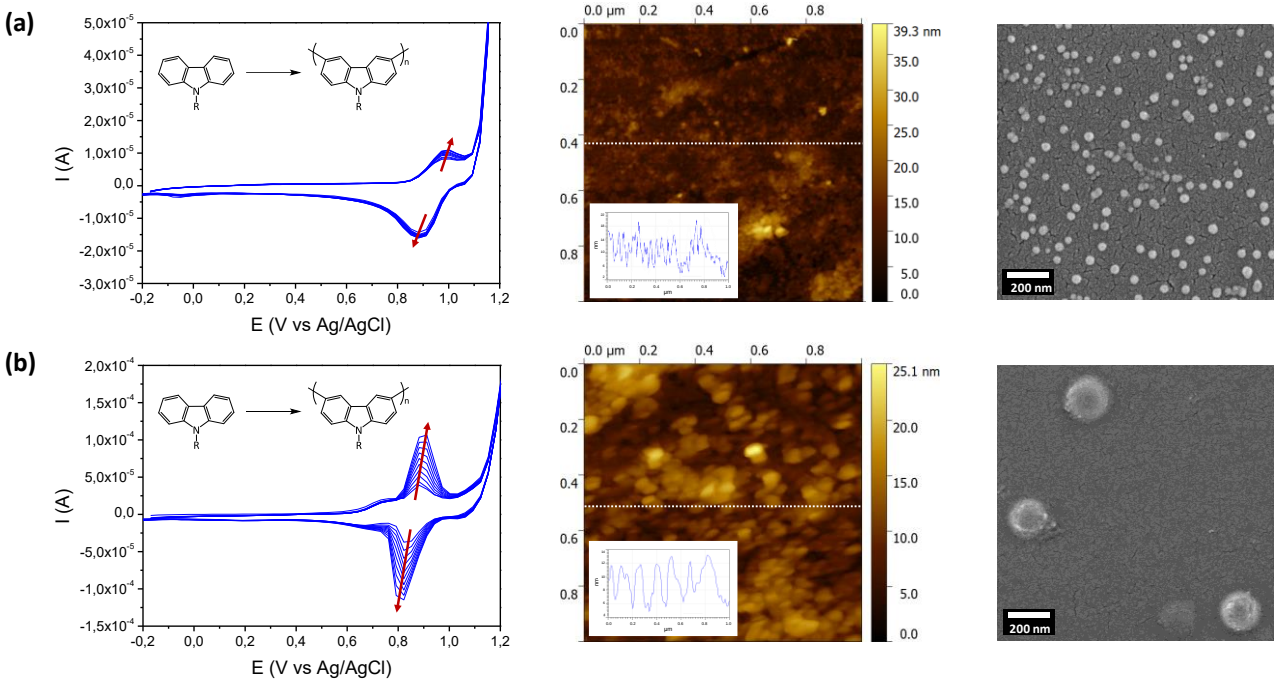

Figure 5. Cyclic voltammograms (100 mV/s, 10 cycles) of the electrochemical polymerization (left), tapping-mode AFM topography images (middle), and SEM images (right) of the electropolymerized films domains from: **(a) dPhCz**, and **(b) ZnP-dPhCz**.

Upon further cycling in CV experiments, it is possible to induce an electropolymerization of carbazole units due to inter- and intramolecular crosslinking at the 3,6-positions to form poly(3,6-carbazole) derivatives with great potential for producing electro-optical materials.[33-36] Therefore, we carried out electrochemical crosslinking of carbazole units on ITO substrates from the precursor azido-functionalized dendrons (**dCz** and **dPhCz**) and the porphyrin-core dendrimers (**ZnP-dCz** and **ZnP-dPhCz**). In all cases, 10 cyclic voltammetry (CV) cycles were applied by scanning the electrodes from -0.2 to 1.2 V. Cyclic voltammograms are shown in **Figure 5**, with the arrows pointing from the 1st to the 10th cycle.

In the first cycle of **ZnP-dPhCz**, the onset of porphyrin and carbazole oxidation was found at around 0.63 and 0.79 V, respectively. **dPhCz** exhibited one oxidation peak at 0.85 V corresponding to carbazole units. Starting from the second CV cycle, the oxidation waves ranged from 0.8 to 1.0 V corresponded to the doping process of the polymerized carbazoles and the formation of polaronic and bipolaronic species.[37] The reduction peaks from 1.0 to 0.7 V corresponded to the dedoping process, in which the polarons and bipolarons gained electrons to give the neutral coupled carbazole species.[37] Upon further cycling, the oxidation and reduction currents increased progressively, indicating a continous mass deposition of **dPhCz** and **ZnP-dPhCz** with more charges built up in the electropolymerized films. The anodic and cathodic currents of **dPhCz** were significally lower than those of **ZnP-dPhCz** due to the lower number of active species (carbazole) per molecule. Nevertheless, in **ZnP-dPhCz**, which has a higher number of carbazole moieties per molecule, the anodic and cathodic peaks moved further apart with increasing CV cycles. This suggests that more **ZnP-dPhCz** was electrochemically deposited onto the electrodes. On the other hand, **dCz** and **ZnP-dCz** were not electrochemically deposited onto ITO electrodes, as deduced from the CV voltammograms (**Figure S10**). These compounds have 3-substituted carbazole units and consequently, the coupling of carbazoles at 3,6-position and subsequent polymerization is not expected.

Crosslinking of the peripheral carbazoles at the 3,6-position leads to the formation of electrodeposited materials onto ITO electrodes. Their morphology was studied by using AFM measurements (**Figure 5**). In the case of **dPhCz**, small globular particles (<40 nm) were formed, while for the porphyrin-core dendrimer (**ZnP-dPhCz**), the size increased up to 150 nm. The increasing number of electropolymerizable units has a decisive influence on the final size of the particles. An increase of the number of cycles (up to 20) does not modify the size of the particles, which suggests that the equilibrium is readily achieved. The morphology of **dPhCz** and **ZnP-dPhCz** after electrochemical deposition onto ITO electrodes was also studied by SEM to confirm agreement with the AFM measurements. As shown in **Figure 5**, the size of the globular particules was found to be around 50 nm (for **dPhCz**) and 170 nm (for **ZnP-dPhCz**).

Charge Transport Properties

The charge carrier mobility measurements were performed by using the space charge-limited current (SCLC) technique. For this purpose, it is necessary to have an ohmic contact between the semiconductor and the injecting electrode. Specifically, in the case of hole conductors the energy level of the HOMO (the LUMO for electron conductors) and the work function of the injecting electrode should not differ by more than ~ 0.3 eV.

Considering the HOMO energy value of the materials ($E_{HOMO} \approx -5.0$ eV) and the work function of Au ($W_{Au} \approx -5.1$ eV), Au was chosen for the injecting electrode to ensure the formation of

an ohmic contact. As a counter-electrode, ITO was used because its work function (W_{ITO} ≈ – 4.6 eV) is significantly lower than the estimated LUMO of the semiconductor (E_{LUMO} ≈ – 3.0 eV), and thus the contribution to the measured current from electrons should be negligible. As detailed in the Supporting Information, in the current-voltage measurements, at low fields, the observed current is ohmic and shows a linear dependence on the applied field, while at higher fields the current may become space-charge limited, showing a different dependence. In this regime, charge mobilities can be obtained from *J–V* curves.

In thick samples (7–12 μm), high currents with only a linear dependence on the applied field (ohmic regime) were observed for **ZnP-dPhCz**, even at the highest applied electric fields, and the SCLC regime was not achieved, probably because the injected charges never reached a density high enough for the set-up of the space-charge regime. Only in a single area of a single sample of **ZnP-dPhCz** the SCLC regime was obtained (Figure S12 in the SI), and thus mobility could be measured, an area where the current was particularly low, probably a consequence of a more disordered environment. In contrast, measurements on samples of **ZnP-dCz** did not show the same problem; a typical J/V curve of the SCLC regime is shown in Figure S11 of the SI. It should be pointed out that the mobility values extracted from SCLC measurements suffer from being model dependent. Measurements as a function of sample thickness could help to establish the reliability of results.[38, 39] As described in the Supporting Information, thinner samples were prepared but no SCLC regime was observed for either compound. As a consequence, the values that were measured should only be considered as an estimate of the order of magnitude of hole mobility.

The estimated hole mobility for **ZnP-dCz** is μ~0.5 ± 0.4 $cm^2V^{-1}s^{-1}$. In the case of **ZnP-dPhCz**, as already explained and detailed in the Supporting Information, a reliable measurement could not be performed, but the high currents, compared to those measured for similar samples of **ZnP-dCz**, hint at even higher mobility values. These hole mobilities are on the higher end of the spectrum, when compared to those reported so far in the literature for purely organic columnar LCs (in the range of 10^{-2}-1 $cm^2{\cdot}V^{-1}{\cdot}s^{-1}$),[10, 15] and are of the same order of magnitude as those found in columnar metallomesogens (values around 1-10 $cm^2{\cdot}V^{-1}{\cdot}s^{-1}$).[12] We note that the results reported here are particularly relevant as those semiconducting LCs with high hole mobility exhibited highly ordered columnar organizations. However, the introduction of the carbazole units does not introduce a significant increase in the hole mobility, when comparing with values obtained using coumarin analogues.[24] These results confirm the importance the central metal-porphyrin core in determining the phase structure, charge mobility and the alignment on surfaces. The spontaneous homeotropic alignment, with its very low density of defects, seems to play a fundamental role for inducing such high hole mobility values, more than the intrinsic contribution of the peripheral functional units.

Conclusions

In conclusion, we have prepared a new family of disk-like liquid crystalline dendrimers with a porphyrin core and carbazole units at the periphery. All the compounds displayed a high HOMO energy level (of around –5.0 eV). Notably, we have demonstrated that it is possible to deposit spherical nanoparticles on ITO electrodes *via* electrochemical crosslinking of peripheral carbazole units. The high HOMO level and the electrodeposited films are promising features and make these dendrimers suitable for optoelectronics applications. Moreover, these carbazole-containing porphyrin-core dendrimers displayed nematic discotic LC phases and are stable up to 300 °C. In this anisotropic arrangement, the compounds can be easily processed as thin film and show a high tendency to form large, defect-free homeotropic domains. Charge mobility studies revealed that these dendrimers in the frozen discotic nematic mesophase displayed semiconductor properties with very high hole mobility.

Conflicts of interest

There are no conflicts to declare.

Acknowledgements

This work was supported by the MINECO-FEDER funds (PGC2018-097583-B-I00) and Gobierno de Aragón-FEDER (Research Group E47_17R). RT was supported by the MERAVIGLIE project (CUP J28C17000080006). Authors would like to acknowledge the use of the SAI (UZ) and CEQMA (UZ-CSIC) Services.

References

1. P. van der Asdonk and P. H. J. Kouwer, Liquid crystal templating as an approach to spatially and temporally organise soft matter, *Chem. Soc. Rev.*, **2017**, *46*, 5935-5949.
2. T. Kato, J. Uchida, T. Ichikawa and T. Sakamoto, Functional Liquid Crystals towards the Next Generation of Materials, *Angew. Chem. Int. Ed.*, **2018**, *57*, 4355-4371.
3. A. Concellón, C. A. Zentner and T. M. Swager, Dynamic Complex Liquid Crystal Emulsions, *J. Am. Chem. Soc.*, **2019**, *141*, 18246-18255.
4. A. H. Gelebart, D. Jan Mulder, M. Varga, A. Konya, G. Vantomme, E. W. Meijer, R. L. B. Selinger and D. J. Broer, Making waves in a photoactive polymer film, *Nature*, **2017**, *546*, 632-636.
5. D. J. Broer, C. M. W. Bastiaansen, M. G. Debije and A. P. H. J. Schenning, Functional Organic Materials Based on Polymerized Liquid-Crystal Monomers: Supramolecular Hydrogen-Bonded Systems, *Angew. Chem. Int. Ed.*, **2012**, *51*, 7102-7109.
6. T. Kato, M. Yoshio, T. Ichikawa, B. Soberats, H. Ohno and M. Funahashi, Transport of ions and electrons in nanostructured liquid crystals, *Nat. Rev. Mater.*, **2017**, *2*, 17001.
7. M. Mathews and Q. Li, in *Self-Organized Organic Semiconductors*, John Wiley & Sons, Inc., 2011, DOI: 10.1002/9780470949122.ch4, pp. 83-129.
8. W. Pisula and K. Müllen, in *Handbook of Liquid Crystals*, eds. J. W. Goodby, P. J. Collings, T. Kato, C. Tschierske, H. Gleeson and P.

Raynes, Wiley-VCH Verlag GmbH & Co. KGaA, Second edn., 2014, vol. 8, ch. 20, pp. 627-673.
9. T. Wöhrle, I. Wurzbach, J. Kirres, A. Kostidou, N. Kapernaum, J. Litterscheidt, J. C. Haenle, P. Staffeld, A. Baro, F. Giesselmann and S. Laschat, Discotic Liquid Crystals, *Chem. Rev.*, **2016**, *116*, 1139-1241.
10. J. De, I. Bala, S. P. Gupta, U. K. Pandey and S. K. Pal, High Hole Mobility and Efficient Ambipolar Charge Transport in Heterocoronene-Based Ordered Columnar Discotics, *J. Am. Chem. Soc.*, **2019**, *141*, 18799-18805.
11. B. Feringán, P. Romero, J. L. Serrano, C. L. Folcia, J. Etxebarria, J. Ortega, R. Termine, A. Golemme, R. Giménez and T. Sierra, H-Bonded Donor–Acceptor Units Segregated in Coaxial Columnar Assemblies: Toward High Mobility Ambipolar Organic Semiconductors, *J. Am. Chem. Soc.*, **2016**, *138*, 12511-12518.
12. R. Chico, E. de Domingo, C. Domínguez, B. Donnio, B. Heinrich, R. Termine, A. Golemme, S. Coco and P. Espinet, High One-Dimensional Charge Mobility in Semiconducting Columnar Mesophases of Isocyano-Triphenylene Metal Complexes, *Chem. Mater.*, **2017**, *29*, 7587-7595.
13. W. Pisula, X. Feng and K. Müllen, Tuning the Columnar Organization of Discotic Polycyclic Aromatic Hydrocarbons, *Adv. Mater.*, **2010**, *22*, 3634-3649.
14. C.-X. Liu, H. Wang, J.-Q. Du, K.-Q. Zhao, P. Hu, B.-Q. Wang, H. Monobe, B. Heinrich and B. Donnio, Molecular design of benzothienobenzothiophene-cored columnar mesogens: facile synthesis, mesomorphism, and charge carrier mobility, *J. Mater. Chem. C*, **2018**, *6*, 4471-4478.
15. A. Benito-Hernández, U. K. Pandey, E. Cavero, R. Termine, E. M. García-Frutos, J. L. Serrano, A. Golemme and B. Gómez-Lor, High Hole Mobility in Triindole-Based Columnar phases: Removing the Bottleneck of Homogeneous Macroscopic Orientation, *Chem. Mater.*, **2013**, *25*, 117-121.
16. C. Tschierske, Development of Structural Complexity by Liquid-Crystal Self-assembly, *Angew. Chem. Int. Ed.*, **2013**, *52*, 8828-8878.
17. T. Kato, N. Mizoshita and K. Kishimoto, Functional liquid-crystalline assemblies: Self-organized soft materials, *Angew. Chem. Int. Ed.*, **2006**, *45*, 38-68.
18. B. M. Rosen, C. J. Wilson, D. A. Wilson, M. Peterca, M. R. Imam and V. Percec, Dendron-Mediated Self-Assembly, Disassembly, and Self-Organization of Complex Systems, *Chem. Rev.*, **2009**, *109*, 6275-6540.
19. S. Hernández-Ainsa, M. Marcos and J. L. Serrano, in *Handbook of Liquid Crystals*, eds. J. W. Goodby, P. J. Collings, T. Kato, C. Tschierske, H. Gleeson and P. Raynes, Wiley-VCH Verlag GmbH & Co. KGaA, Second edn., 2014, vol. 7, ch. 7, pp. 259-300.
20. M. Marcos, R. Martín-Rapún, A. Omenat and J. L. Serrano, Highly congested liquid crystal structures: dendrimers, dendrons, dendronized and hyperbranched polymers, *Chem. Soc. Rev.*, **2007**, *36*, 1889-1901.
21. H. J. Sun, S. Zhang and V. Percec, From structure to function via complex supramolecular dendrimer systems, *Chem. Soc. Rev.*, **2015**, *44*, 3900-3923.
22. V. Iguarbe, A. Concellón, R. Termine, A. Golemme, J. Barberá and J. L. Serrano, Making Coaxial Wires Out of Janus Dendrimers for Efficient Charge Transport, *ACS Macro Lett.*, **2018**, *7*, 1138-1143.
23. A. Concellón, R. Termine, A. Golemme, P. Romero, M. Marcos and J. L. Serrano, High hole mobility and light-harvesting in discotic nematic dendrimers prepared via 'click' chemistry, *J. Mater. Chem. C*, **2019**, *7*, 2911-2918.
24. A. Concellón, M. Marcos, P. Romero, J. L. Serrano, R. Termine and A. Golemme, Not Only Columns: High Hole Mobility in a Discotic Nematic Mesophase Formed by Metal-Containing Porphyrin-Core Dendrimers, *Angew. Chem. Int. Ed.*, **2017**, *56*, 1259-1263.
25. H. Vedala, Y. Chen, S. Cecioni, A. Imberty, S. Vidal and A. Star, Nanoelectronic Detection of Lectin-Carbohydrate Interactions Using Carbon Nanotubes, *Nano Letters*, **2011**, *11*, 170-175.
26. E. Blasco, J. L. Serrano, M. Piñol and L. Oriol, Light responsive vesicles based on linear–dendritic block copolymers using azobenzene–aliphatic codendrons, *Macromolecules*, **2013**, *46*, 5951-5960.
27. M. Arseneault, C. Wafer and J. F. Morin, Recent Advances in Click Chemistry Applied to Dendrimer Synthesis, *Molecules*, **2015**, *20*, 9263.
28. S. Guerra, T. L. A. Nguyen, J. Furrer, J.-F. Nierengarten, J. Barberá and R. Deschenaux, Liquid-Crystalline Dendrimers Designed by Click Chemistry, *Macromolecules*, **2016**, *49*, 3222-3231.
29. A. Lancelot, R. González-Pastor, A. Concellón, T. Sierra, P. Martín-Duque and J. L. Serrano, DNA Transfection to Mesenchymal Stem Cells Using a Novel Type of Pseudodendrimer Based on 2,2-Bis(hydroxymethyl)propionic Acid, *Bioconjugate Chemistry*, **2017**, *28*, 1135-1150.
30. S. Hecht, N. Vladimirov and J. M. J. Fréchet, Encapsulation of Functional Moieties within Branched Star Polymers: Effect of Chain Length and Solvent on Site Isolation, *J. Am. Chem. Soc.*, **2001**, *123*, 18-25.
31. A. Adronov, S. L. Gilat, J. M. J. Fréchet, K. Ohta, F. V. R. Neuwahl and G. R. Fleming, Light Harvesting and Energy Transfer in Laser−Dye-Labeled Poly(aryl ether) Dendrimers, *J. Am. Chem. Soc.*, **2000**, *122*, 1175-1185.
32. S. L. Gilat, A. Adronov and J. M. J. Fréchet, Light Harvesting and Energy Transfer in Novel Convergently Constructed Dendrimers, *Angew. Chem. Int. Ed.*, **1999**, *38*, 1422-1427.
33. P. F. Cao, L. H. Rong, A. de Leon, Z. Su and R. C. Advincula, A Supramolecular Polyethylenimine-Cored Carbazole Dendritic Polymer with Dual Applications, *Macromolecules*, **2015**, *48*, 6801-6809.
34. C. Kaewtong, G. Jiang, M. J. Felipe, B. Pulpoka and R. Advincula, Self-Assembly and Electrochemical Oxidation of Polyamidoamine−Carbazole Dendron Surfmer Complexes: Nanoring Formation, *ACS Nano*, **2008**, *2*, 1533-1542.
35. P. Taranekar, T. Fulghum, D. Patton, R. Ponnapati, G. Clyde and R. Advincula, Investigating Carbazole Jacketed Precursor Dendrimers: Sonochemical Synthesis, Characterization, and Electrochemical Crosslinking Properties, *J. Am. Chem. Soc.*, **2007**, *129*, 12537-12548.
36. P. Taranekar, J. Y. Park, D. Patton, T. Fulghum, G. J. Ramon and R. Advincula, Conjugated Polymer Nanoparticles via Intramolecular Crosslinking of Dendrimeric Precursors, *Adv. Mater.*, **2006**, *18*, 2461-2465.
37. G. Jiang, R. Ponnapati, R. Pernites, C. D. Grande, M. J. Felipe, E. Foster and R. Advincula, Nanoparticle Formation and Ultrathin Film Electrodeposition of Carbazole Dendronized Polynorbornenes Prepared by Ring-Opening Metathesis Polymerization, *Langmuir*, **2010**, *26*, 17629-17639.
38. J. C. Blakesley, F. A. Castro, W. Kylberg, G. F. A. Dibb, C. Arantes, R. Valaski, M. Cremona, J. S. Kim and J.-S. Kim, Towards reliable charge-mobility benchmark measurements for organic semiconductors, *Org. Electron.*, **2014**, *15*, 1263-1272.
39. M. Zubair, Y. S. Ang and L. K. Ang, Thickness Dependence of Space-Charge-Limited Current in Spatially Disordered Organic Semiconductors, *IEEE Transactions on Electron Devices*, **2018**, *65*, 3421-3429.